31st Annual International Conference of the IEEE EMBS
Minneapolis, Minnesota, USA, September 2-6, 2009

Experimental Characterization of a Vector Doppler System Based on a Clinical Ultrasound Scanner

Avinash Eranki and Siddhartha Sikdar, *Member, IEEE*

Abstract— **We have developed a vector Doppler system using a clinical ultrasound scanner with a research interface. In this system, vector Doppler estimation is performed by electronically dividing a linear array transducer into a transmit sub-aperture and two receive sub-apertures. The receive beams are electronically steered, and two velocity components are estimated from echoes received from the beam overlap region. The velocity vector is reconstructed from these two estimates. The goal of this study was to characterize this vector Doppler system *in vitro* using a string phantom with a pulsatile velocity waveform. We studied the effect of four parameters on the estimation error: beam steering angle, angle of the velocity vector, depth of the scatterer relative to the beam overlap region and the transmit focus depth. Our results show that changing these parameters have minimal effect on the velocity and angle estimates, and robust velocity vector estimates can be obtained under a variety of conditions. The mean velocity error was less than 0.06 × pulse repetition frequency. The velocity estimates are sensitive to the Doppler estimation method. Our results indicate that vector Doppler using a linear array transducer is feasible for a wide range of imaging parameters. Such a system would facilitate the investigation of complex blood flow and tissue motion in human subjects.**

Keywords-Ultrasonography, pulsed Doppler, vector Doppler; blood flow velocity, tissue motion, array transducers, signal processing;

I. Introduction

Doppler ultrasound (US) is a widely used diagnostic tool. One inherent problem with Doppler US is that only motion along the axis of the beam can be detected. This poses a problem estimating the true velocity of blood flow or tissue motion, which occurs in 3D. In the clinic, B-mode imaging is used to visualize the angle of the vessel and an angle correction factor is applied [1]. Flow is assumed to be laminar along the vessel axis. This assumption may not be valid for complex flows [2]. Furthermore, for tissue Doppler imaging (TDI) the direction of motion may not be known a priori. Ultrasound methods for estimating true 3D velocities could lead to better assessment of complex blood flow and 3D tissue motion.

Vector Doppler is one method to estimate blood flow and tissue velocities in two or more independent directions using multiple US transmitters and receivers [3]. The vector Doppler method combines multiple received velocity components to obtain a velocity vector with magnitude and direction. Various vector Doppler methods have been proposed that use different configurations of transmitters and receivers [4-9]. Several groups have developed custom vector Doppler systems using multiple transducers.

Another approach to vector Doppler is to use a clinical system with an array transducer and electronically split the aperture to form multiple transmit and receive sub-apertures, which can then be steered in different directions [10, 11]. This flexible approach has the advantage of electronically controlling the transmitter and receiver geometry and the ability to perform experiments in a clinical setting with simultaneous imaging. However, vector Doppler systems based on array transducers have not been extensively investigated. We have developed a vector Doppler system based on a clinical scanner with a research interface. The goal of this paper is to investigate the robustness of the velocity vector estimates to change in parameters like beam steering angle, velocity vector angle, depth of the scatterer relative to the beam overlap region, and depth of transmit focus, and validate the measurements using a Doppler string phantom.

II. Methods & Materials

A. Vector Doppler system design

The vector Doppler method is based on estimating the flow vector from measurements taken from two or more independent directions. These independent velocity estimates can then be used to reconstruct the velocity vector. We accomplished this on a clinical scanner with an array transducer using the setup shown in Fig 1. The array transducer was divided into a transmit sub-aperture and two receive sub-apertures. Ultrasound is transmitted along a beam normal to the transducer. The receive apertures are steered at an angle, β, relative to the normal. This vector Doppler configuration was implemented on an Ultrasonix SonixRP US system (Richmond, BC, Canada) with a 5-14 MHz linear array probe, L14-5/38, with a 38-mm field of view consisting of 128 elements. The SonixRP system has a research interface that enables low-level beam forming and pulse sequencing control through a software development kit called Texo. We used this interface to split the array transducer into sub-apertures and steer the receive beams. The transmit and receive beams overlap as shown in Fig. 1. To increase the size of the overlap region, the transmit beam is focused at a point farther than the region of interest, essentially making the beam un-focused at the region of interest. The receive beams are focused dynamically.

Estimation of the velocity vector using the configuration shown in Fig. 1 has been described previously [4]. For a velocity vector of magnitude, v, at an angle, θ, to the normal, the Doppler frequency estimated using the echoes from the

A.Eranki and S. Sikdar are with the Department of Electrical and Computer Engineering and Krasnow Institute for Advanced Study, George Mason University, Fairfax, VA 22030 USA. Corresponding author: S. Sikdar (phone: 703-993-1539; e-mail: ssikdar@ gmu.edu).

first receive aperture and the second receive aperture is given by:

$$v_1 = v\cos(\theta) + v\cos(\theta - \beta) \qquad (1)$$

$$v_2 = v\cos(\theta) + v\cos(\theta + \beta) \qquad (2)$$

where v = velocity along the transmit beam; β = receive beam steering angle; θ = angle between the transmit beam and the velocity vector.

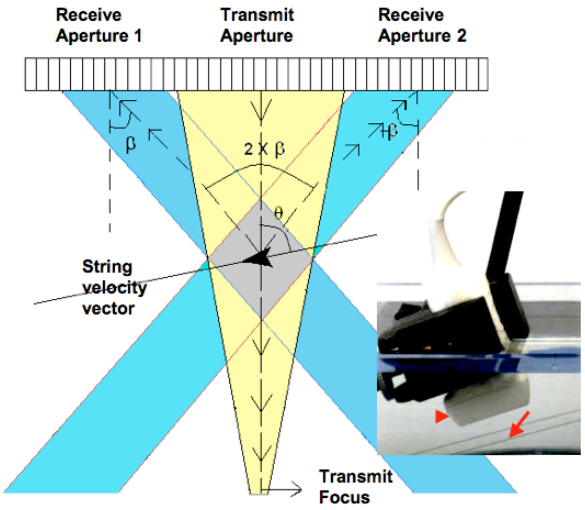

Figure 1.Vector Doppler geometry showing the transmit aperture (yellow) and the receive apertures (blue). Inset image shows the experimental setup. The arrowhead points to the transducer and the arrow points to the string driven by the motor.

Using (1) and (2), we obtain the velocity, v, and angle θ:

$$v = \sqrt{\left(\frac{v_1 + v_2}{2(1+\cos\beta)}\right)^2 + \left(\frac{v_1 - v_2}{2(\sin\beta)}\right)^2}; \theta = \tan^{-1}\left[\frac{1+\cos\beta}{\sin\beta} \cdot \frac{v_1 - v_2}{v_1 + v_2}\right] \quad (3)$$

B. *in vitro* Validation Studies

A calibrated Doppler string phantom (CIRS, Norfolk, VA, USA) was used for evaluating the accuracy of velocity vector estimation. The experimental setup consists of a string (surgical 3-0 suture) attached to a stepper motor-driven pulley. The motor drive is programmable and can produce different string velocity waveforms. The transducer was positioned at different orientations by a clamp. The transducer and string were immersed in an acrylic water bath. Our experiments used the preset string velocity waveform for the common carotid artery.

The B-mode image was used to position the probe and measure the depth and orientation of the string relative to the transducer to accuracy of 0.1 mm and +/- 2^0, respectively. The pulse repetition frequency (PRF) was 10.44 KHz, transmit frequency was 5 MHz, and the transmit and receive apertures were 32 elements wide. The following four parameters were varied to investigate their effect on the estimation error of the velocity vector: (1) receive beam steering angle, (2) depth of string (3) velocity vector angle and (4) depth of transmit focus. An ideal velocity waveform was generated based on the string phantom specifications.

C. Data analysis

The raw RF data were digitized at 40-MHz and analyzed offline using MATLAB (Mathworks, Inc., Natick, MA). The data were demodulated to baseband and filtered with a 100-Hz high pass filter to remove stationary and low-frequency clutter. Mean velocities were estimated using the conventional autocorrelation velocity estimator [12] with an ensemble size of 48. A correction term (equal to one standard deviation) was added to the velocity to better estimate the Doppler spectral envelope. A median filter was employed to remove isolated velocity peaks. Noise was removed using a threshold of -6dB from the peak power signal. The velocity vector was reconstructed using Eq. 3 and compared with an ideal velocity waveform based on the string phantom specifications.

III. Results

RF data were collected for a total of 33 *in vitro* tests for scenarios described in Section II.B. The velocity magnitudes and directions were estimated. Fig. 2 shows the vector Doppler displays for β = 45 and θ = 90 & 75 respectively. The Doppler spectrograms for each receive aperture, corresponding to the velocity estimates in Eqs. (1) and (2), were used to reconstruct the estimated string velocity vector. The estimated velocity vectors are shown for different orientations of the string, demonstrating angle-independent velocity estimation.

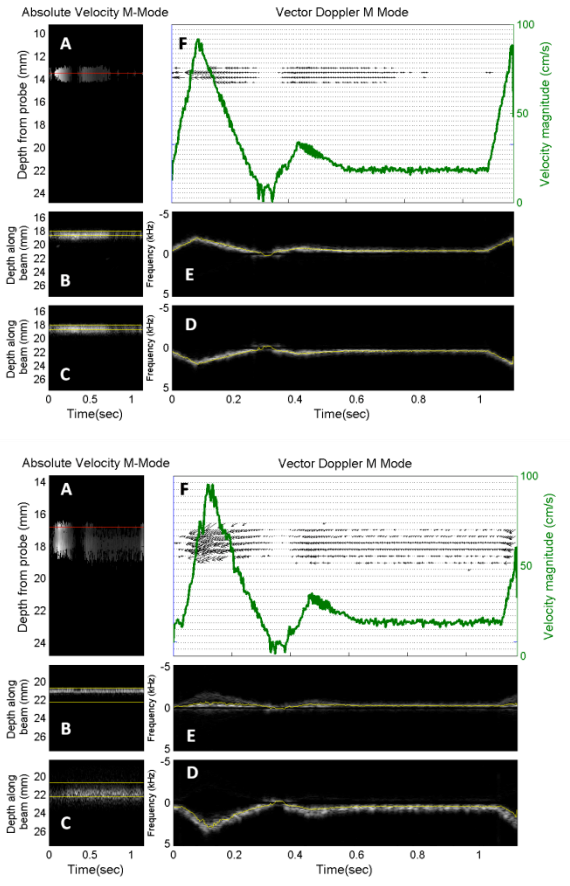

Figure.2 Vector Doppler displays for β = 45 and θ = 90 (top panel) and β= 45 and θ = 75 (bottom panel). (a) The velocity magnitude displayed as an M-mode. (b), (c) Echo M-mode with depth along the steered receive beam for receive apertures 1 and 2, respectively. (d), (e) The spectrogram of the received echoes from the region of interest for each receive apertures 1 and 2, respectively. (f) Velocity M-mode with arrows showing the flow vector.

Table1.
Dependence of the estimated mean peak systolic velocity and angle estimates on the steering angle, focusing depth, depth and orientation of the string.

Scenarios	Steering angle, β (deg.)	Transmit focus depth (mm)	String angle, θ (deg.)	String depth (mm)	Mean abs. error in velocity (cm/s)	Standard deviation of error in velocity (cm/s)	Max abs error in velocity (cm/s)	Mean abs error in angle (deg.)	Standard deviation of error in angle (deg.)
1	15 (center of beam overlap: 22 mm)	12	90	23	9.64	9.94	43.76	2.84	1.26
2		23	90	23	7.00	9.29	39.20	2.75	1.15
3		40	90	23	8.30	9.40	42.21	2.17	2.15
4		60	90	16	4.74	3.97	20.28	0.72	1.03
5				18	5.39	2.99	16.02	0.55	0.42
6				20	7.40	4.07	23.51	0.67	0.49
7				22	9.22	4.56	26.28	0.73	0.88
8			75	16	8.48	5.23	25.34	4.64	1.9
9				18	6.39	3.83	23.61	3.78	1.99
10				20	6.73	4.13	18.80	4.16	2.57
11				22	5.33	4.15	27.36	3.1	2.12
12	30 (center of beam overlap: 21 mm)	12	90	23	7.14	4.79	23.36	1.56	1.05
13		23	90	23	8.08	5.50	29.60	1.23	0.88
14		40	90	23	3.09	3.15	16.77	1.77	0.88
15		60	90	16	2.16	2.56	13.12	0.93	1.14
16				18	3.70	2.85	20.90	0.68	0.59
17				20	3.53	2.36	12.93	0.99	1.3
18				22	5.69	5.07	29.40	0.82	0.56
19			75	16	8.67	4.91	25.09	1.85	1.23
20				18	6.52	4.11	26.11	5.37	2.59
21				20	6.06	4.27	21.81	3.37	2.18
22				22	5.04	5.11	26.41	4.76	2.41
23	45 (center of beam overlap: 12 mm)	12	90	18	5.58	3.26	19.71	2.44	3.52
24		18	90	18	7.71	5.45	26.90	0.84	0.97
25		30	90	18	4.38	3.92	16.35	1.89	0.67
26		60	90	12	2.56	2.53	11.95	0.23	0.24
27				14	3.52	3.67	19.75	0.4	0.39
28				16	5.85	4.08	22.27	0.51	0.48
29				18	9.37	6.28	31.04	0.56	0.75
30			75	12	3.66	4.03	20.95	5.06	3.49
31				14	2.80	2.27	10.80	4.39	2.2
32				16	2.95	3.00	16.63	8.33	2.46
33				18	4.66	4.85	30.01	6.13	1.22

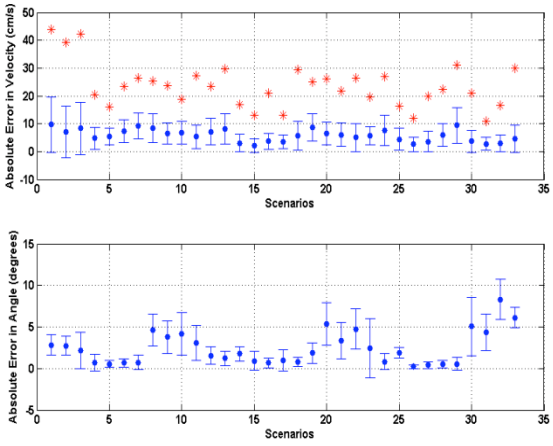

Figure.3. Mean absolute error plots for velocity (top panel) and angle (bottom panel) estimates. The error bars represent standard deviations. The maximum absolute velocity error is indicated in red. The scenarios refer to column # 1 in Table 1.

Table 1 and Figure 3 summarize the estimation errors for different experimental conditions. The velocity estimation errors were calculated by comparing the estimates with the ideal velocity waveform based on the string phantom specification. Although the errors are comparable for different scenarios, the largest velocity errors occurred for the 15^0 steering. This is expected, since the Doppler shifts for both receive apertures are lower in this scenario. The maximum velocity errors tend to occur near velocity maxima (within 0.1 sec of the velocity peak in 19 out of 33 scenarios) or minima (within 0.1 sec of the velocity trough in 6 out of 33 scenarios).

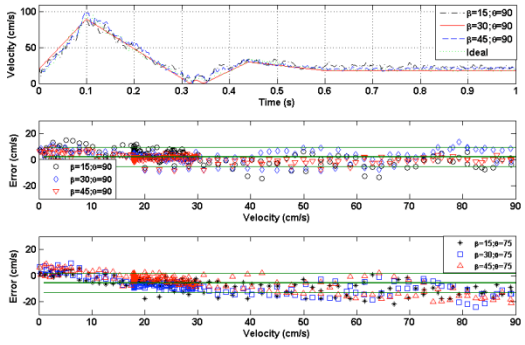

Figure.4. Estimated velocity waveforms for three different steering angles compared to the ideal velocity waveform (top panel). Bland-Altman plots for different beam steering angles with $\theta = 90^0$ (middle panel) and $\theta = 75^0$ (bottom panel). Green lines are mean±1.96×standard deviation.

Figure 4 shows that the estimated velocity waveforms for different beam steering angles are similar to the ideal waveform, and the velocity estimation errors are similar, although the velocity tends to be underestimated for 75^0 beam to string angle.

IV. Discussion

We characterized the accuracy of a vector Doppler system based on a clinical US scanner with an array transducer for estimating the velocity magnitude and direction. We investigated the effect of four factors: (1) the beam steering angle, (2) the angle of the velocity vector, (3) the depth of the scatterer relative to the beam overlap region and (4) the transmit focus depth.

Each of the above four parameters were varied keeping the other three parameters constant, as shown in Table 1. Our results indicate that the estimation errors are largely unaffected by the choice of the imaging system parameters. As expected, the maximum errors in velocity magnitude occurred for the 15^0 beam steering. Beam steering has been shown to cause errors in 1D pulsed Doppler [13], however we did not observe any major differences in estimation error for 30^0 and 45^0 steering. The errors increased somewhat as the string was moved farther from the center of the beam overlap region. The mean errors were typically less than 10 cm/s (or 0.06×PRF), independent of the depth. These errors are similar to those reported in the literature [11].

The errors were sensitive to the method used for velocity estimation. The conventional autocorrelation method underestimated the velocities, especially during peak acceleration. After adding a variance correction term, the mean absolute estimation error decreased, while the maximum velocity errors increased for some scenarios. We believe that the maximum errors near velocity maxima were caused by increased variance due to spectral broadening, while those near the velocity minima were due to the suppression of low velocities by the clutter filter. More sophisticated velocity estimators can decrease the maximum errors. In this study, we did not investigate the impact of grating lobes due to beam steering. This will be addressed in future studies.

In this study, we utilized a single transmit aperture and two separate receive apertures. Other configurations are possible, such as two transmit and receive apertures [4, 11]. With our configuration, the path length of the ultrasound beam between transmit and receive is smaller than in the latter case, and the transmit path is shared between the receive apertures. We believe that this configuration would minimize any effects due to differences in the intervening tissues along the two paths.

A major advantage of using a linear array imaging transducer for performing vector Doppler is the ability to electronically control the receive beam steering, and aperture locations, for scanning a large field of view. Furthermore, duplex and triplex vector Doppler is possible, and conventional B-mode and color Doppler can be used to locate the region of interest for quantification of vector flow and tissue motion. While other researchers have utilized linear arrays for vector Doppler [10,11], the effect of imaging parameters, such as beam steering and transmit defocusing have not been investigated. Our results demonstrate that vector Doppler imaging using a linear array transducer is feasible for a wide range of imaging parameters and can be used for several *in vivo* investigations.

V. Conclusion

We have developed a vector Doppler system using a clinical US scanner. Using this system, we have characterized the accuracy of vector Doppler *in vitro* using a string phantom. Our results show that the effect of beam steering and transmit beam defocusing do not have a significant effect on the estimation of velocities. Velocity estimation errors increase somewhat as we move farther from the region of overlap of the beams, and as the angle between the receive beams decrease. With further refinement, this technique can improve the precision of Doppler velocimetry, as well as enable assessment of muscle contraction velocities in patients with movement and neuro-muscular disorders.

References

[1] W.M. Blackshear Jr., D.J. Phillips, B.L. Thiele, J.H. Hirsch, P.M. Chikos, M.R.Marinelli, K.J. Ward and D.E. Strandess Jr., "Detection of carotid occlusive disease by ultrasonic imaging and pulsed Doppler analysis," *Surgery*, pp. 698-706, Nov., 1979.

[2] W. D. Middleton, W. D. Foley and T.L Lawson, "Color-flow Doppler imaging of carotid artery abnormalities," *American Roen. Ray Society.*,pp. 419-425, 1988.

[3] P.L Hansen, G. Cross, L. H. Light, "Beam-angle independent Doppler velocity measurement in superficial vessels," In: *Woodcock JP, ed. Clinical Blood flow measurement,* London: Sector Publishing, pp. 28-32, 1974

[4] B. Dunmire, K. W. Beach, K-H. Labs, M. Plett and D.E. Strandess Jr., "Cross-beam vector Doppler ultrasound for angle-independent velocity measurements," *Ultrasound Med. Biol.,* vol. 26, pp. 1213-1235, 2000.

[5] O. D. Kripfgans, J. M. Rubin, A. L. Hall and J. B. Fowlkes, "Vector Doppler imaging of a spinning disc ultrasound Doppler phantom," *Ultrasound Med. Biol.,* vol. 32, pp. 1037-1046, 2006.

[6] R. Steel, K. V. Ramnarine, F. Davidson, P. J.Fish and P. R. Hoskins, "Angle-independent estimation of maximum velocity through stenosis using vector Doppler," *Ultrasound Med. Biol.,* vol. 29, pp. 575-584, 2003.

[7] R. Steel, K. V. Ramnarine, A. Criton, F. Davidson, P.L. Allan, N. Humphries, H.F Routh, P.J Fish and P. R.Hoskins, "Angle-independence and reproducibility of dual-beam vector Doppler ultrasound in the common carotid arteries of normal volunteers," *Ultrasound Med. Biol.,* vol. 30, pp. 271-276, 2004.

[8] P.R. Hoskins, "A comparison of single- and dual-beam methods for maximum velocity estimation," *Ultrasound Med. Biol.,* vol. 25, pp. 583-592, 1999.

[9] J.R. Overbeck, K.W. Beach, D.E. Strandness Jr., "Vector Doppler: accurate measurement of blood velocity in two dimensions," *Ultrasound Med. Biol.,* vol. 18(1), pp. 19-31, 1992.

[10] M. Scabia, M. Calzolai, L. Capineri, l. Masotti and A. Fort, "A real-time two-dimensional pulsed wave Doppler system," *Ultrasound Med. Biol.,* vol. 26, pp. 121-131, 2000.

[11] A. Pastorelli, G. Torricelli, M. Scabia, E. Biagi and l. Masotti, "A real-time 2-D vector Doppler system for clinical experimentation," *IEEE Trans. Med. Imag*., vol.27, pp. 1515-1524, 2008.

[12] C. Kasai, K. Namekawa, A. Koyano and R. Omoto, "Real-time two-dimensional blood flow imaging using autocorrelation technique," *IEEE Trans. Sonics Ultrasonics*, vol. Su-32, pp.458-464, 1985.

[13] A. H. Steinman, A. C. H. Yu, K. W. Johnston and R. S.C. Cobbold, "Effects of beam steering in pulsed-wave ultrasound velocity estimation," *Ultrasound Med. Biol.,* vol. 31, pp. 1073-1082, 2005.